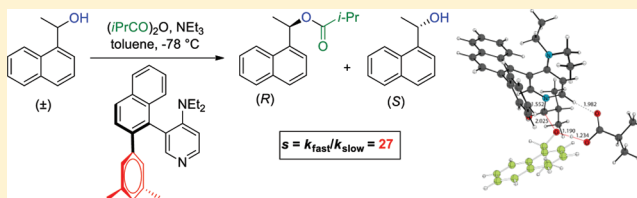


## Theoretical Prediction of Selectivity in Kinetic Resolution of Secondary Alcohols Catalyzed by Chiral DMAP Derivatives

Evgeny Larionov,<sup>†,||</sup> Mohan Mahesh,<sup>‡,§</sup> Alan C. Spivey,<sup>\*,‡</sup> Yin Wei,<sup>†,⊥</sup> and Hendrik Zipse<sup>\*,†</sup><sup>†</sup>Department of Chemistry, LMU München, Butenandtstrasse 5-13, D-81377 München, Germany<sup>‡</sup>Department of Chemistry, South Kensington Campus, Imperial College, London, SW7 2AZ, United Kingdom

## Supporting Information

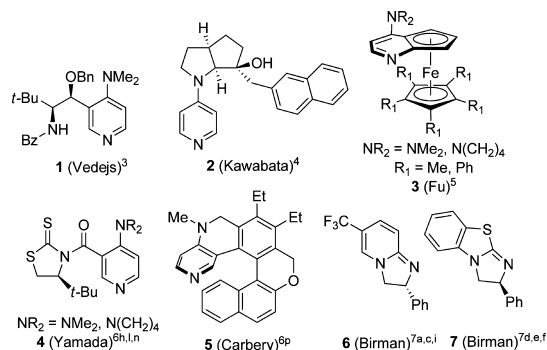
**ABSTRACT:** The mechanism of esterification of the secondary alcohol 1-(1-naphthyl)ethanol **9** by isobutyric anhydride catalyzed by 4-pyrrolidinopyridine (PPY, **11**) and a series of single enantiomer atropisomeric 4-dialkylaminopyridines **8a–g** has been studied computationally at the B3LYP/6-311+G(d,p)//B3LYP/6-31G(d) level. Comparison of the levels of enantioselectivity predicted computationally with the results obtained experimentally allowed the method to be validated. The value of the approach is demonstrated by the successful prediction that a structural modification of an aryl group within the catalyst from phenyl to 3,5-dimethylphenyl would lead to improved levels of selectivity in this type of kinetic resolution (KR) reaction, as was subsequently verified following synthesis and evaluation of this catalyst (**8d**). Experimentally, the selectivity of this type of KR is found to exhibit a significant deuterium isotope effect (for **9** vs **d**<sub>1</sub>-**9**).



## INTRODUCTION

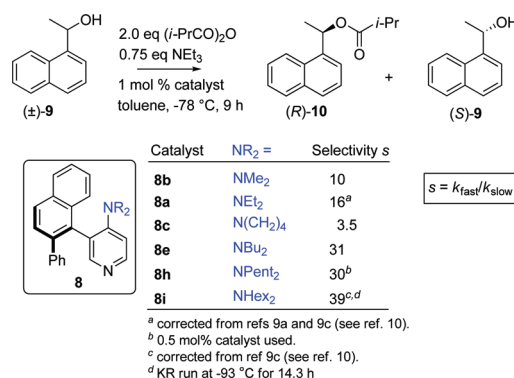
Organocatalysis has been at the forefront of research in organic chemistry in recent years, and one of the most studied fields concerns acyl group transfer reactions mediated by nucleophilic chiral catalysts.<sup>1</sup> Structurally diverse amine, phosphine, and alcohol derivatives have been designed and synthesized for the kinetic resolution (KR) of alcohols and related stereoselective transformations.<sup>2</sup> In particular, chiral 4-dimethylamino-pyridine (DMAP) derivatives **1–5** have been demonstrated to be effective catalysts for enantioselective acyl-transfer reactions to alcohols by Vedejs,<sup>3</sup> Kawabata,<sup>4</sup> Fu,<sup>5</sup> and others.<sup>6</sup> Additionally, Birman<sup>7</sup> and others<sup>8</sup> have demonstrated that various bicyclic amidines (e.g., **6** and **7**) are highly effective catalysts for this type of transformation (Chart 1).

Chart 1. Representative Structures of 4-DMAP and Amidine-Based Catalysts Used for the KR of Alcohols



Spivey et al. have also developed a series of axially chiral, atropisomeric derivatives of 4-dialkylaminopyridines **8** as catalysts for the KR of racemic secondary alcohols (Scheme 1).<sup>9</sup>

Scheme 1. KR of Alcohol **9** by Isobutyrylation, Catalyzed by Atropisomeric DMAP Derivatives **8**<sup>9c</sup>



These experiments were performed using racemic 1-(1-naphthyl)ethanol **9** as the substrate and isobutyric anhydride (1 equiv) as acyl donor in the presence of 1 mol % of the enantiomerically pure biaryl catalysts **8**. Under these conditions, the alcohol (*R*)-**9** reacts faster than the alcohol (*S*)-**9** to produce ester (*R*)-**10**, and a selectivity factor *s* = 16 was obtained using the 4-diethylamino catalyst (–)-(*S*<sub>a</sub>)-**8a** at –78 °C.<sup>9c,10</sup> In a similar manner, KR experiments performed using

Received: March 12, 2012

Published: May 8, 2012

atropisomeric derivatives having various 4-dialkylamino groups revealed that the selectivities (and activities) of these catalysts depend on the nature of this group with the 4-di-*n*-butyl derivative **8e** showing the optimal combination of selectivity and activity.<sup>9c</sup> These findings motivated us to perform a combined theoretical and experimental investigation to better understand the acylation reaction of racemic alcohols and the factors influencing the selectivities of these catalysts.

Currently, only a small number of theoretical studies have been reported in which not only conformational properties of the acylpyridinium intermediates have been studied<sup>14a,11</sup> but also direct prediction of the outcome of KR experiments with alcohols has been attempted. These studies deal, however, with chiral imidazole and amidine derivatives. Sunoj et al.<sup>12a</sup> have studied computationally the enantioselective acetylation of *trans*-cyclohexane-1,2-diol, catalyzed by a *N*-methylimidazole-based peptide, which was designed by Schreiner et al.<sup>12b</sup> These authors have shown that hydrogen bonding between the diol substrate and the peptide backbone plays an important role in determining the enantioselectivity. Analysis of the transition-state structures for the acylation of 1-phenylethanol catalyzed by amidine **6** (Chart 1), carried out by Houk et al., supports the decisive role of  $\pi$ - $\pi$  interactions in mediating chiral recognition in the KR of secondary benzylic alcohols.<sup>7h</sup>

With the aim to improve our understanding of the relationship between catalyst structure and the level of enantioselectivity imparted during chiral DMAP catalysis of acyl-transfer reactions to the point where predictions can be made, we have investigated computationally the acylation of the racemic secondary alcohol 1-(1-naphthyl)ethanol **9** catalyzed by the series of catalysts **8** in detail. The key question here is whether the enantioselectivities of chiral DMAP-catalyzed acyl-transfer reactions can be rationalized by examination of the transition state (TS) of the rate-determining step that is also considered as the selectivity-determining step.

## COMPUTATIONAL DETAILS

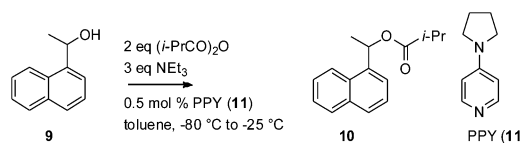
All conformers of reactants and products were searched carefully and optimized at the B3LYP/6-31G(d) level, and single point calculations were added at the B3LYP/6-311+G(d,p) level of theory in order to obtain relative enthalpies at B3LYP/6-311+G(d,p)//B3LYP/6-31G(d) level. The systems studied here are very flexible and have a large conformational space. The conformational spaces of transition states **TS1** and **TS2** for the 4-pyrrolidinopyridine (PPY) catalyst (**11**) and 4-diethylaminopyridine catalyst **8a** were initially studied with the optimized potentials for liquid simulations (OPLS)-AA force field using the Monte Carlo conformational search facility implemented in BOSS 4.6.<sup>12</sup> The conformational space of transition state **TS2** for catalysts **8b** and **8c** was also initially studied with the OPLS-AA force field.<sup>13</sup> The conformers identified by the force field within an energy window of 40 kJ mol<sup>-1</sup> were then reoptimized at the B3LYP/6-31G(d) level of theory, and single point calculations were carried out at the B3LYP/6-311+G(d,p) level of theory. Intrinsic reaction coordinate (IRC) calculations were executed using the lowest-energy conformers of these TSs to obtain structures of the reactant complex, the intermediate acylpyridinium salt (pyac) on the nucleophilic catalysis pathway, and the product complex. The transition states **TS3** and **TS4** for catalysts PPY (**11**) and **8a** on the base-catalyzed pathway were located based on the previously suggested “four-” and “six-membered” ring structures<sup>14</sup> and optimized at the B3LYP/6-31G(d) level.

Single point calculations were again performed at the B3LYP/6-311+G(d,p) level of theory as well as at MP2(FC)/6-311+G(d,p) and MP2(FC)/6-31+G(2d,p) levels with Gaussian 03.<sup>15</sup> Dispersion corrections to the DFT (termed DFT-D) proposed by S. Grimme<sup>16</sup> were used to calculate the accurate dispersion interaction at the B3LYP-D/6-311+G(d,p) level using the ORCA 2.6.4 program package.<sup>17</sup> Thermochemical corrections to free energies and enthalpies at 298.15 K ( $G_{298}$  and  $H_{298}$ ) as well as at 195.15 K ( $H_{195}$  and  $G_{195}$ ) were calculated at the same level as that used for geometry optimization.

## RESULTS AND DISCUSSION

**Catalysis by PPY.** Catalyst **8a** has been shown to be very effective for the KR of secondary alcohols.<sup>9</sup> However, the selectivity values can vary slightly as a function of conversion:  $s = 16.7$  at 12% conversion (2 h) using 1 equiv anhydride and  $s = 15.9$  at 27% conversion (8 h) with 1 equiv anhydride (for the reaction shown in Scheme 1, see Supporting Information).<sup>10</sup> There are also several communications of the conversion-dependent selectivity in the literature.<sup>18</sup> Additionally, it was noted, that the reaction mixture at  $-78$  °C is not homogeneous, while at room temperature no precipitation was observed.<sup>9d</sup> This phenomenon may be explained by the formation of insoluble triethylammonium salts (in toluene), which can in principle affect the reaction (rate or/and selectivity). Should this be the case, we must expect that the Arrhenius plot for the reaction rate or even selectivity will not necessarily remain linear. In order to understand the role of precipitation, we decided to study the reaction kinetics at different temperatures. As a model system, the isobutyrylation of racemic 1-(1-naphthyl)ethanol **9** catalyzed by PPY (**11**) was chosen (Scheme 2).

**Scheme 2.** Isobutyrylation of 1-(1-Naphthyl)ethanol **9**, Catalyzed by PPY (**11**)



This reaction follows second-order kinetics, and rate constants were measured at eight different temperatures from  $-25$  °C to  $-80$  °C. In order to determine the activation parameters, the obtained data were fitted using the Eyring equation (Figure 1).

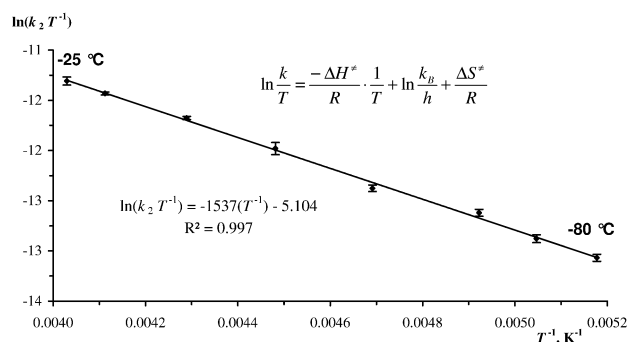


**Figure 1.** Eyring plot for the reaction shown in Scheme 2.

The value obtained for the activation enthalpy  $\Delta H^\ddagger$  of 12.8 kJ mol<sup>-1</sup> (Table 1) is quite small for a reaction in solution,

**Table 1. Comparison of Activation Parameters for the Acylation of Alcohol 9 Catalyzed by PPY (11)**

activation parameter	exp <sup>a</sup>	TS1•9 <sup>b</sup>	TS2 <sup>b</sup>	TS2 <sup>c</sup>
$\Delta H^\ddagger$ , kJ mol <sup>-1</sup>	+12.8	+23.8	+11.0	+12.6
$\Delta G^\ddagger$ , kJ mol <sup>-1</sup>	+84.3 <sup>d</sup>	+177.5	+168.3	+118.8
$\Delta S^\ddagger$ , J mol <sup>-1</sup> K <sup>-1</sup>	-240	-788	-806	-356

<sup>a</sup>Experimental values from the Eyring plot from 193 to 248 K.

<sup>b</sup>Activation parameters of TS1•9 and TS2 calculated at B3LYP/6-311+G(d,p)//B3LYP/6-31G(d) level at 195 K. <sup>c</sup>Calculated at 298 K. <sup>d</sup>At 298 K.

whereas the negative value obtained for the activation entropy  $\Delta S^\ddagger$  of -240 J mol<sup>-1</sup> K<sup>-1</sup> is typical for a bimolecular reaction.<sup>19,20</sup> By comparison, Vedejs reported that the isobutyrylation of 1-(1-naphthyl)ethanol 9 catalyzed by a chiral phospholane in toluene also had a small activation enthalpy ( $\Delta H^\ddagger$  = 5.8 or 12.5 kJ mol<sup>-1</sup>, depending on the reacting enantiomer of 9)<sup>19</sup> and that the activation entropies were similarly large and negative irrespective of the reacting enantiomer of 9 ( $\Delta S^\ddagger$  = -311 or 306 J mol<sup>-1</sup> K<sup>-1</sup>). Vedejs' data imply that the  $\Delta G^\ddagger$  term, which determines enantiomer discrimination, is dominated by differences in activation enthalpies  $\Delta H^\ddagger$ . The kinetic parameters of other acyl-transfer

reactions feature a similar combination of minimal activation enthalpies  $\Delta H^\ddagger$  and large, negative activation entropies  $\Delta S^\ddagger$ .<sup>20</sup>

**Computational Study of the Catalytic Cycle with PPY (11).** The DMAP-catalyzed acylation of alcohols by anhydrides and acyl chlorides is generally believed to proceed via a nucleophilic catalysis mechanism.<sup>1b</sup> This mechanism is supported by the computational study of the DMAP-catalyzed acetylation of *tert*-butanol with acetic anhydride.<sup>14</sup> It has however been noted that in the case of primary alcohols a mechanism involving base catalysis may become competitive.<sup>21</sup> In order to investigate, which mechanism of catalysis (nucleophilic or general base) is operative for the isobutyrylation of secondary alcohol 9 catalyzed by PPY (11), we studied the catalytic cycle computationally. The free energy profile as calculated at the B3LYP/6-311+G(d,p)//B3LYP/6-31G(d) level at the experimental temperature of 195.15 K is shown in Figure 2 (enthalpies  $\Delta H^\ddagger$  and free energies  $\Delta G^\ddagger$  at 298 K are shown in the Supporting Information).

First, the reaction profile was calculated assuming initial formation of a ternary complex of reactants and catalyst PPY (11) for both the nucleophilic and general base catalysis pathways.<sup>14</sup> Along the nucleophilic catalysis pathway, the reactant complex passes through the first transition state TS1•9 to yield intermediate **pyac**•9, which then passes through the second TS2 with concomitant proton transfer to give the product complex. The alternative base catalysis pathway proceeds through the concerted "six-membered" ring TS3 or

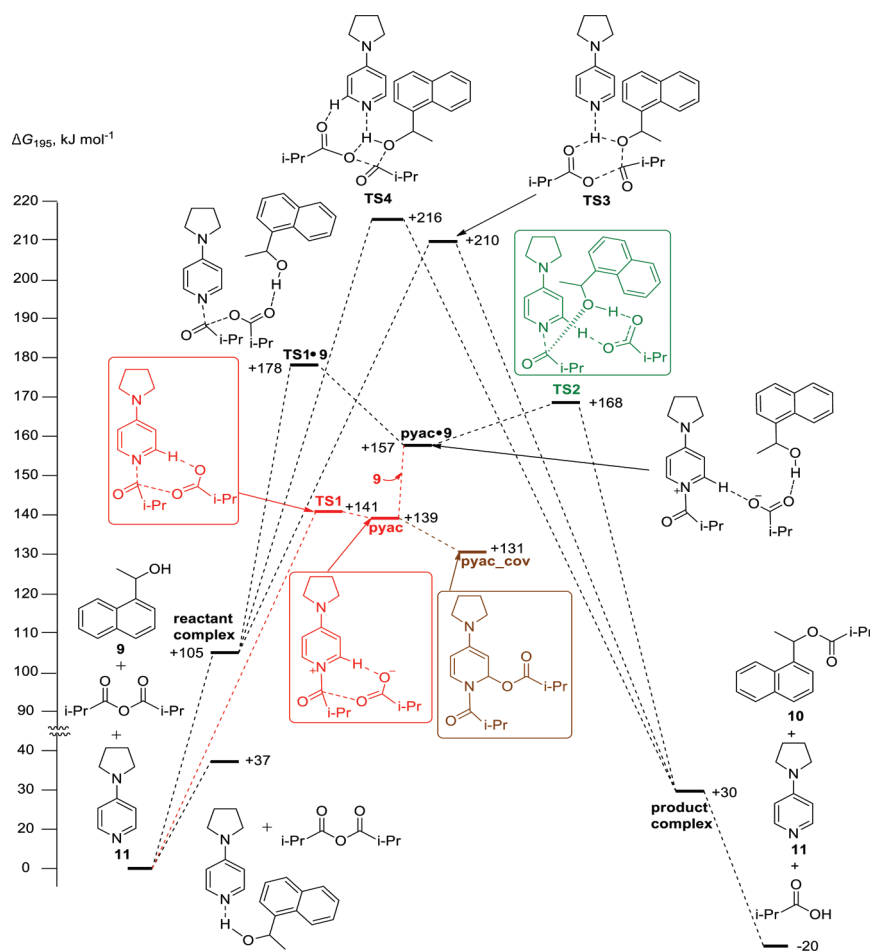


**Figure 2.** Free energy profile ( $\Delta G_{195}$ ) of the PPY-catalyzed acylation of alcohol 9 as calculated at B3LYP/6-311+G(d,p)//B3LYP/6-31G(d) level.

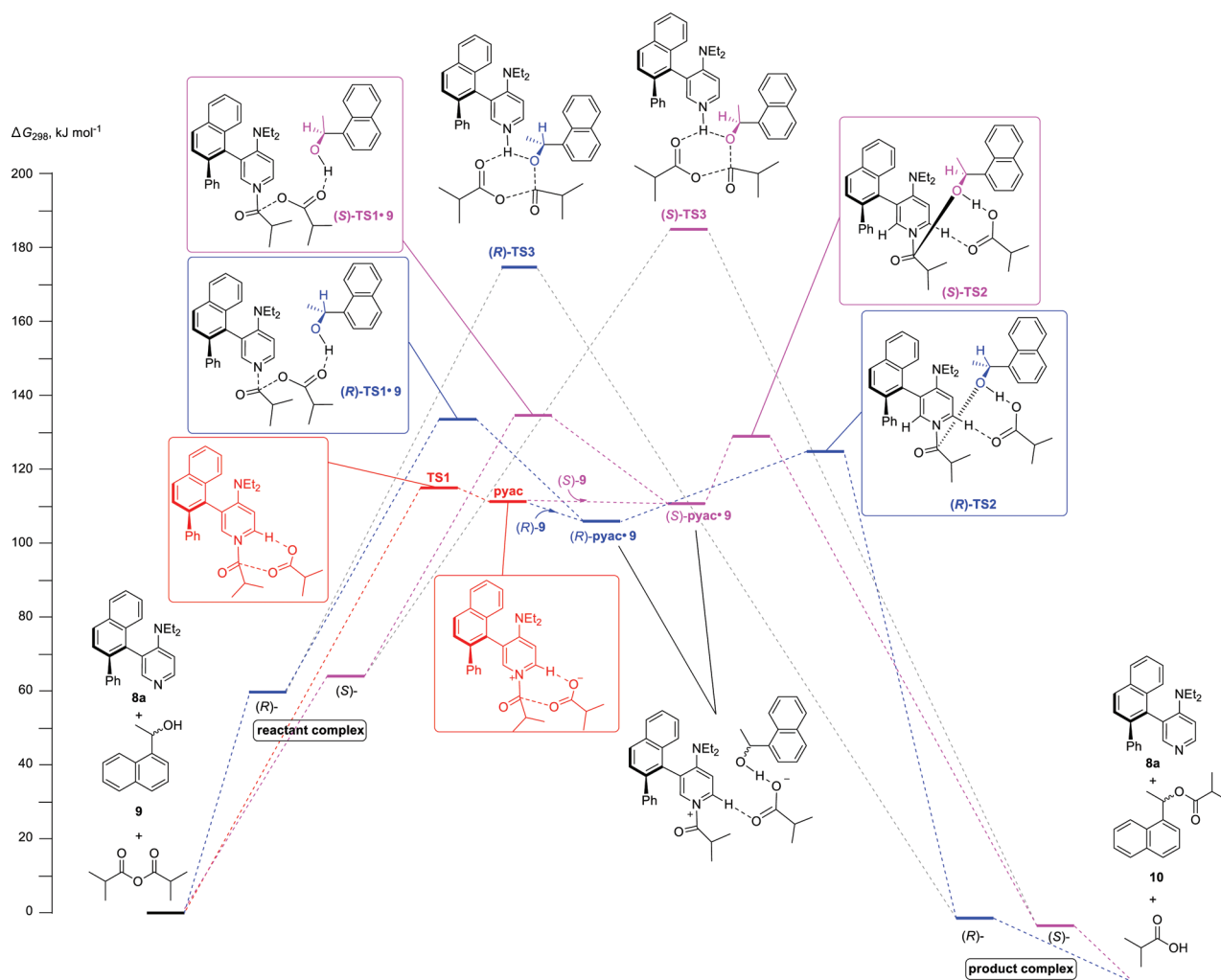


**Figure 3.** Gas-phase free energy profile ( $\Delta G_{298}$ ) of the acylation of alcohol **9** catalyzed by  $(-)-(S_a)$ -**8a** as calculated at the B3LYP/6-311+G(d,p)//B3LYP/6-31G(d) level of theory.

“four-membered” ring **TS4** to the product complex in a single step. The six-membered transition state **TS3** of the base-catalyzed route is slightly more favorable than the four-membered **TS4**. The activation parameters (relative to separate reactants) for transition states **TS1**·**9** and **TS2** calculated at the B3LYP/6-311+G(d,p)//B3LYP/6-31G(d) level of theory are collected in Table 1.

Both enthalpy and free energy values suggest the nucleophilic route to be more favorable and the first step of this route to be rate-limiting. This was surprising, because the second step is generally considered to be rate determining.<sup>1b,14</sup> However, inclusion of the alcohol molecule in the first step appeared to be entropically unfavorable. Therefore an alternative path through **TS1** and intermediate **pyac**, which does not include alcohol **9**, was calculated (marked in red in Figure 2). The new transition state **TS1** without alcohol **9** has a higher enthalpy than **TS1**·**9** but is more stable in terms of free energy. The subsequent intermediate **pyac** can then react with alcohol **9** through **TS2** to give products. Interestingly, the covalently bound dihydropyridine intermediate **pyac\_cov** is slightly more stable than the ion pair **pyac** and may be present in equilibrium with **pyac**. Transition state **TS2** (marked in green in Figure 2) has a higher free energy than **TS1**, and therefore via this nucleophilic catalysis pathway, the second step is rate limiting. The experimental value of the activation enthalpy  $\Delta H^\ddagger$  (+12.8

kJ mol<sup>-1</sup>) is close to the theoretically predicted value for the rate-limiting transition state **TS2** (+12.6 kJ mol<sup>-1</sup> at 298 K, Table 1). The activation entropy of **TS2** (−356 J mol<sup>-1</sup> K<sup>-1</sup> at 298 K) deviates significantly from the experimental value of −240 J mol<sup>-1</sup> K<sup>-1</sup>. These latter deviations (cf.,  $\Delta G_{\text{exp}}^\ddagger$  84.3 vs  $\Delta G_{\text{calc}}^\ddagger$  118.8 kJ mol<sup>-1</sup>) may be due to the presently employed harmonic oscillator/rigid rotor model for thermal corrections.

In order to test whether these observations persist at other theoretical levels, additional single point calculations were performed using the B3LYP/6-31G(d) structures. The MP2 method as well as the DFT method with dispersion correction (DFT-D)<sup>16</sup> were chosen in combination with the 6-311+G-(d,p) basis set due to their superior performance in describing dispersion interactions. The results show that the use of MP2 and B3LYP-D levels for single point calculations stabilizes all the TSs relative to the reactants and reactant complex (see Supporting Information). All these different theoretical methods predict the base-catalyzed route to be less favorable than the nucleophilic route (by ca. 30–40 kJ mol<sup>-1</sup>). Transition states of the base-catalyzed route, **TS3** and **TS4**, have similar energies at different levels of theory and are therefore equally feasible for the base-catalyzed pathway.

**Computational Study of the Catalytic Cycle with Catalyst  $(-)-(S_a)$ -**8a**.** In order to check whether the



mechanism of the acylation of secondary alcohols catalyzed by PPY (**11**) also persists for the acylation catalyzed by the chiral catalyst  $(-)-(S_a)$ -**8a**, we next investigated the nucleophilic and general base catalysis pathways for the reaction of racemic 1-(1-naphthyl)ethanol (**9**) with isobutyric anhydride catalyzed by  $(-)-(S_a)$ -**8a** also at the B3LYP/6-311+G(d,p)//B3LYP/6-31G(d) level of theory. The nucleophilic and general base catalysis pathways are plotted in Figure 3 using the lowest-energy conformers. The diastereoisomeric TSs and intermediates are denoted as  $(R)^*$  and  $(S)^*$ , depending on the configuration of the involved alcohol.

The diastereoisomers including  $(R)$  alcohol (**9**) are always a few  $\text{kJ mol}^{-1}$  lower than those including the  $(S)$  alcohol. The most energetically favorable transition state  $(R)$ -TS3 along the base catalysis pathway is located  $60 \text{ kJ mol}^{-1}$  above transition state TS1 and  $51 \text{ kJ mol}^{-1}$  above transition state  $(R)$ -TS2 of the nucleophilic catalysis pathway (Table 2). Single point

**Table 2. Relative Enthalpies  $\Delta H_{298}$  and Free Energies  $\Delta G_{298}$  (in  $\text{kJ mol}^{-1}$ ) for Stationary Points Located on the Potential Energy Surface at the B3LYP/6-311+G(d,p)//B3LYP/6-31G(d) Level in the Gas Phase for the Acylation of Alcohol **9** Promoted by Catalyst  $(-)-(S_a)$ -**8a****

	$\Delta H_{298}$		$\Delta G_{298}$	
nucleophilic catalysis	(R)-	(S)-	(R)-	(S)-
reactants	0.0		0.0	
reactant complex	−23.0	−22.5	59.7	64.2
TS1•9	26.8	34.3	133.3	134.2
pyac•9	7.6	11.7	106.3	111.1
TS1	58.7		114.6	
pyac	57.8		110.4	
TS2	14.1	20.1	124.0	129.1
product complex	−87.4	−86.9	−0.7	−4.7
products	−21.6		−19.4	
base catalysis (concerted)	(R)-	(S)-	(R)-	(S)-
TS3	67.2	77.5	175.3	185.7

calculations have also been performed at the MP2/6-31G(d)//B3LYP/6-31G(d) level of theory for the best conformers of the  $(R)$ -TSs (see Supporting Information). The energy of  $(R)$ -TS3 is also higher than that of  $(R)$ -TS1 and  $(R)$ -TS2 by more than  $30 \text{ kJ mol}^{-1}$  at the MP2/6-31G(d)//B3LYP/6-31G(d) level. This indicates that the nucleophilic catalysis pathway is more favorable than the general base catalysis pathway, which is in line with the results for the acylation catalyzed by PPY (**11**) discussed above.

The free energy difference between the diastereoisomeric TSs of the rate-determining step is the key value for predicting the enantioselectivity. In accordance with the results for PPY-catalyzed acylation, the first transition state TS1 has a lower free energy when alcohol **9** is not included in the structure (Table 2). Hence, in the nucleophilic route the reactants pass through the first transition state TS1 to yield intermediate pyac, which is common for both alcohol enantiomers. After complexation with either the  $(R)$  or  $(S)$  alcohol **9**, the  $(R)$ - or  $(S)$ -pyac•**9** intermediates pass through their respective second TS2s to the product complex. Transition state TS2 is rate limiting for both alcohols and should therefore also be selectivity determining. Free activation energies  $\Delta G_{298}$  for the acylation catalyzed by  $(-)-(S_a)$ -**8a** ( $124.0 \text{ kJ mol}^{-1}$  for  $(R)$ -TS2 and  $129.1 \text{ kJ mol}^{-1}$  for  $(S)$ -TS2) are higher than the  $\Delta G_{298}$  value calculated for PPY ( $118.8 \text{ kJ mol}^{-1}$ ). This is in accordance

with experimental observation that PPY (**11**) is more catalytically active than compound **8a**. Furthermore, the free energy difference of  $5.1 \text{ kJ mol}^{-1}$  between  $(R)$ - and  $(S)$ -TS2 is accompanied by an enthalpy difference of  $6.0 \text{ kJ mol}^{-1}$ , confirming that the origin of stereoselection is essentially of enthalpic nature.

Analysis of the optimized geometries of transition states TS2 reveals that all conformers can be classified into one of the four structural types shown in Figure 4, which also shows a pictorial

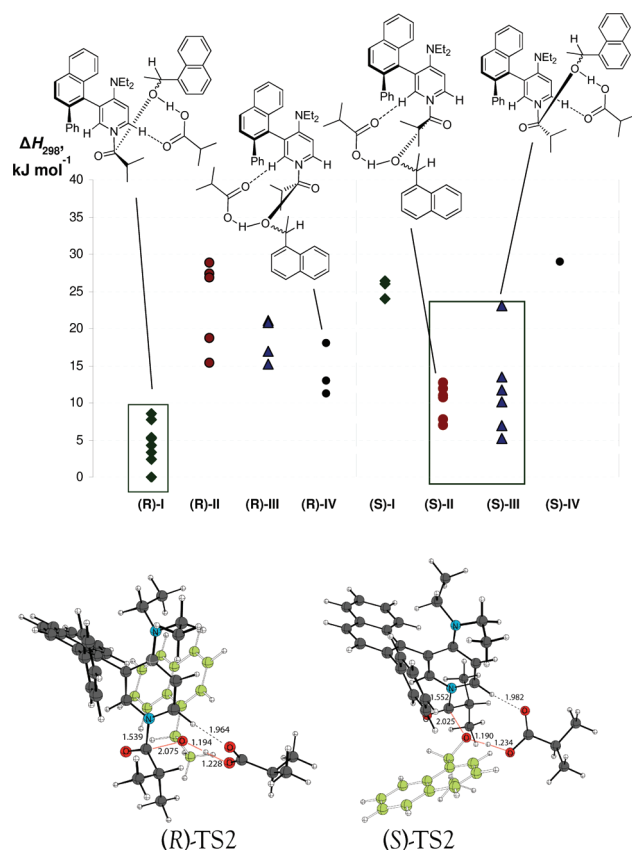


**Figure 4.** Relative enthalpies ( $\text{kJ mol}^{-1}$ ) of conformers of TS2 with catalyst  $(-)-(S_a)$ -**8a** (top) and structures of the most stable conformers of  $(R)$ -TS2 (left bottom) and  $(S)$ -TS2 (right bottom) as calculated at the B3LYP/6-31G(d) level of theory. Each low-energy conformer in classes I–IV is represented by an individual symbol (see Supporting Information for further details). Distances are given in Å.

representation of the relative energies of the conformers of  $(R)$ - and  $(S)$ -TS2. Generally speaking, the carboxyl carbonyl group is bound to the left or right side of the pyridine ring by weak hydrogen bonding, and the alcohol approaches the reaction center from either the front or the back face of the pyridine ring. In class I the carboxylate group is bound to the right side of the pyridine ring, and the alcohol approaches the reaction center from the back. For this class, the conformers with the  $(R)$  alcohol are more stable than the conformers with the  $(S)$  alcohol by more than  $20 \text{ kJ mol}^{-1}$ . In classes II and III the conformers with the  $(S)$  alcohol are more stable than the conformers with the  $(R)$  alcohol. All the conformers in class IV have rather poor stabilities with both the  $(R)$  and the  $(S)$  alcohols. The most stable conformer with the  $(R)$  alcohol belongs to class I, which is more stable than the most stable conformer with the  $(S)$  alcohol (belonging to class III) by  $5.1 \text{ kJ mol}^{-1}$ . Thus, the calculations predict that when employing

Table 3. Comparison of Experimental<sup>9d,10</sup> and Calculated Energy Differences  $\Delta H(S - R)$  and  $\Delta G(S - R)$  (in kJ mol<sup>-1</sup>) of the Diastereoisomers of TS2 for Catalysts 8a–g<sup>a</sup>

catalyst	experiment <sup>b</sup>			B3LYP/6-31G(d) <sup>c</sup>				B3LYP/6-311+G(d,p) <sup>c</sup>		B3LYP-D/6-311+G(d,p) <sup>c</sup>	
	<i>s</i>	ln <i>s</i>	$\Delta G_{195}$	$\Delta G_{298}$	$\Delta H_{298}$	$\Delta G_{195}$	$\Delta H_{195}$	$\Delta G_{298}$	$\Delta H_{298}$	$\Delta G_{298}$	$\Delta H_{298}$
8a	16	2.77	4.49	4.19	5.35	6.77	5.48	5.65	6.13	6.09	1.42
8b	10	2.30	3.73	3.67	4.62	5.33	4.80	5.60	6.12	1.93	1.45
8c	3.5	1.25	2.03	8.23	3.99	8.32	4.31	9.90	5.82	4.18	0.17
8e	31	3.43	5.56	10.27	5.70	8.29	5.75	11.99	6.01	15.30	9.49
correlation coefficient $R^2$ <sup>d</sup>				0.0224	0.9641	0.0011	0.9485	0.0205	0.3987	0.5509	0.6496
8d	27	3.30	5.35	8.23	6.72	6.26	6.70	14.06	9.29	2.13	4.50
8f	11	2.40	3.89	4.78	4.41	4.76	4.51	7.01	6.14	5.85	4.22
8g	9	2.20	3.57	3.98	2.12	2.74	2.11	7.37	5.04	0.91	-0.98
correlation coefficient $R^2$ <sup>e</sup>				0.0967	0.4702	0.0103	0.3975	0.1812	0.2667	0.2307	0.5666

<sup>a</sup>Positive numbers imply a preference for (*R*) alcohol. <sup>b</sup>Selectivities *s* are taken from the experimental results from ref 9c for catalysts 8b, 8c, and 8e (all using 2 equiv anhydride, *t* = 9 h) or were recorded in this work for catalysts 8a,<sup>10</sup> 8d, 8f, and 8g (all using 1 equiv anhydride, *t* = 8 h, see Supporting Information). <sup>c</sup>Level of theory used for single point calculations based on B3LYP/6-31G(d) geometries and thermal corrections. Energy values are Boltzmann-averaged over the maximum available number of conformers (the actual numbers of conformers used for averaging are shown in the Supporting Information). <sup>d</sup>Correlation of the calculated energy differences  $\Delta H(S - R)$  and  $\Delta G(S - R)$  with experimental values ln *s* for catalysts 8a–c and 8e. <sup>e</sup>Correlation of the calculated energy differences  $\Delta H(S - R)$  and  $\Delta G(S - R)$  with experimental values ln *s* for all studied catalysts 8a–g.

(–)-(S<sub>a</sub>)-8a as the KR catalyst, the (*R*) alcohol 9 should react faster than the corresponding (*S*) alcohol, which is in line with experimental observation.<sup>9</sup>

The B3LYP/6-31G(d) optimized structures of the most stable conformers of (*R*)- and (*S*)-TS2 as shown in Figure 4 illustrate that alcohol 9 (shown in light green) approaches the reaction center from the back face of the pyridine ring in (*R*)-TS2 and from the front face of the pyridine ring in (*S*)-TS2. There is no significant steric hindrance when the alcohol approaches the reaction center from the back face of the pyridine in (*R*)-TS2. In contrast, alcohol approaching from the front face of the pyridine in (*S*)-TS2 encounters some steric repulsion between the tilted phenyl ring of the catalyst 8a and the naphthyl ring of alcohol 9, thus raising the energy of (*S*)-TS2 relative to that of (*R*)-TS2 by ca. 5 kJ mol<sup>-1</sup>.

**The Origin of Selectivity: Variations of the Dialkylamino Group.** Spivey et al. have shown experimentally that varying the 4-dialkylamino substituent significantly influences the selectivities of catalysts.<sup>9c</sup> The selectivities decreases in the order 8e, 8a, 8b, 8c, with pyrrolidino-substituted catalyst 8c being the least selective (see Scheme 1). We therefore chose to investigate theoretically the selectivities of the catalyst series 8a–8e using the same alcohol [1-(1-naphthyl)ethanol, 9] as substrate in order to compare to the experimental results. The enthalpy and free energy differences between the diastereoisomers of TS2, which were considered to be the selectivity-determining TSs, were calculated for catalysts 8a–c and 8e by DFT methods and are listed in Table 3.

The calculated free energy differences  $\Delta G_{298}$  for TS2 for catalysts 8a–c and 8e calculated at B3LYP/6-31G(d) level did not reproduce experimental values of  $\Delta G_{195}$ , calculated using eq 1; indeed, they predict that the pyrrolidino-substituted catalyst 8c should have higher selectivity than both 8a and 8b (Table 3). However, the calculated enthalpy differences  $\Delta H_{298}$  do correlate with experimental selectivities quite closely (Figure 5, blue line, correlation coefficient  $R^2 = 0.9641$  for catalysts 8a–c and 8e). The thermal corrections recalculated at 195 K do not improve the correlation between experimental results and calculated free energies or enthalpies (Table 3). In general, enthalpy and free energy differences between (*R*)- and (*S*)-TS2 for catalysts 8a–c and 8e calculated at the B3LYP/6-31G(d)

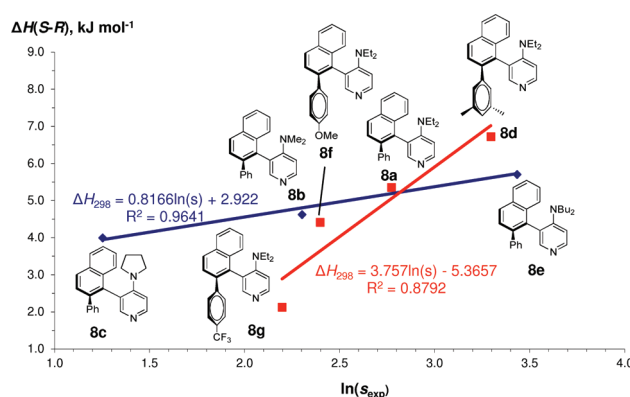


Figure 5. Correlation between experimental enantioselectivities and calculated enthalpy differences  $\Delta H_{298}$  between (*R*)- and (*S*)-TS2, as calculated at the B3LYP/6-31G(d) level.

level predict the (*R*) alcohol to be more reactive than the (*S*) alcohol, which is in full agreement with experimental results.

$$\ln s = \ln \frac{k_R}{k_S} = -\frac{\Delta \Delta G_{195}^\ddagger}{RT} = \frac{\Delta G_S^{\text{TS}} - \Delta G_R^{\text{TS}}}{RT} = \frac{\Delta G^{\text{TS}}}{RT} \quad (1)$$

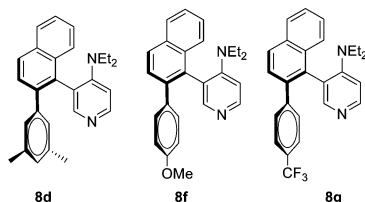
Employing the combined DFT method B3LYP/6-311+G-(d,p)//B3LYP/6-31G(d) also does not yield a better correlation of experimental selectivities with calculated free energies or enthalpies (Table 3). The inclusion of dispersion corrections (at B3LYP-D/6-311+G(d,p) level), however, improves the correlation with calculated free energies. Moreover, after addition of the dispersion corrections, the enthalpy differences  $\Delta H_{298}$  are significantly smaller. Noticeably, the enthalpy differences  $\Delta H_{298}$  between (*R*)- and (*S*)-TS2 for catalysts 8a–c and 8e calculated at the B3LYP-D/6-311+G-(d,p)//B3LYP/6-31G(d) level can be correlated with experimental enantioselectivities (Table 3, correlation coefficient  $R^2 = 0.6496$  for catalysts 8a–c and 8e). Hence it is apparent that enthalpy differences  $\Delta H_{298}$  between (*R*)- and (*S*)-TS2 for catalysts 8a–c and 8e calculated at the B3LYP/6-31G(d) or the combined B3LYP-D/6-311+G(d,p)//B3LYP/6-31G(d) levels

can be used for the rationalization of experimentally measured enantioselectivities in KR experiments.

Comparison of TS structures for **8a** vs **8e**, i.e., containing  $\text{NEt}_2$  vs  $\text{NBU}_2$  groups, respectively, reveals what appear to be only small differences, of which the slightly more advanced proton transfer between alcohol and carboxylate counterion in the (R)-TS2(**8e**) is the most notable stabilizing feature (see Supporting Information). That the butyl substituents in catalyst **8e** interact differently with the surrounding biaryl  $\pi$ -systems in TSs of the (R)- and (S)-alcohols can be seen in the calculations exploring the effects of dispersion corrections. Only for catalyst **8e** can we observe an increase in the predicted selectivity on inclusion of dispersion corrections (Table 3). The proposed dihedral angles of the biaryl bonds in the TSs for **8a** and **8e** differ by less than  $2^\circ$ , suggesting that this is not the origin of the observed selectivity differences in this series of catalysts.

**Selectivity Predictions for KR of Alcohol 9 with Isobutyric Anhydride Catalyzed by Catalysts with Alternative 'Blocking Groups' (8d, 8f, and 8g).** Having established a correlation between computed and experimentally determined selectivities for KR of alcohol **9** by known catalysts **8a**–**c** and **8e**, we were motivated to predict the expected selectivities for the KR of alcohol **9** by a set of unknown derivatives of catalyst **8a** containing different substituents in the phenyl ring, i.e., 3,5-dimethyl- (**8d**), 4-methoxy- (**8f**), and 4-trifluoromethyl substitution (**8g**) (Chart 2). These derivatives

**Chart 2. New Chiral Pyridine Derivatives 8d, 8f, and 8g Used To Model KR of Secondary Alcohols<sup>a</sup>**



<sup>a</sup>All catalysts have (*S<sub>a</sub>*)-configuration.

were selected to assess the roles of steric bulk, electron donation and electron withdrawal, respectively, on the effectiveness of this 'blocking group' within the catalyst structure. The plan was to calculate the relevant enthalpy differences  $\Delta H(S - R)$  between diastereomeric TS2s for each catalyst **8d**, **8f**, and **8g** and then to prepare and test the new catalysts experimentally.

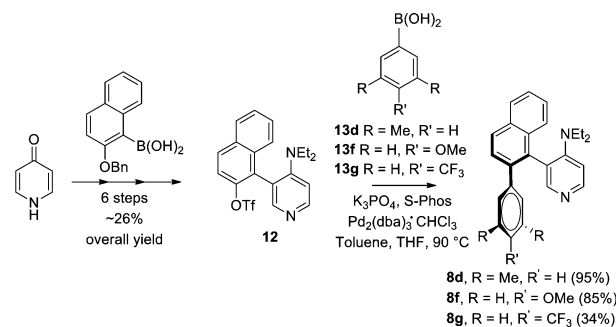
In order to reduce the computational effort, it was considered desirable not to carry out the full conformational search for each new TS2 but rather to use the conformations obtained for TS2 with the parent catalyst **8a** as a basis in each case. The envisaged variations of the catalyst structure were not anticipated to dramatically change the conformational space of TS2. Thus, taking the optimal conformations of TS2 for catalyst **8a**, introducing the modified aryl substituents, and then reoptimizing the TSs at the B3LYP/6-31G(d) level would avoid a lengthy conformational search. Detailed analysis of the conformational space of TS2 (see Supporting Information) shows that taking into account type I conformations for (R)-TS2 and both types II and III for (S)-TS2 is necessary to find the most stable conformations of TS2 (these are marked by green boxes in Figure 4). Moreover, averaging over just the three most stable conformations gives sufficiently accurate enthalpy differences (see Supporting Information for details).

This method was therefore used to calculate enthalpy differences  $\Delta H_{298}(S - R)$  for catalysts **8d**, **8f**, and **8g**, shown in Chart 2. The results obtained for  $\Delta H_{298}(S - R)$  at the B3LYP/6-31G(d) level show that the catalysts **8f** and **8g** are expected to display moderate levels of stereoselectivity, while the derivative **8d** should display greater levels of selectivity relative to the parent catalyst **8a** (see Table 3).

The higher calculated enthalpy difference  $\Delta H_{298}(S - R)$  for catalyst **8d** relative to **8a** can be rationalized by unfavorable interactions between the naphthyl ring system of the (S)-alcohol and one of the methyl groups of the 3,5-dimethylphenyl substituent in the catalyst in (S)-TS2 of type III. This leads to a higher relative stability of the type II conformers (see Supporting Information for further details). For catalysts **8f** and **8g** the para substituents exert no corresponding steric repulsion, and electronic effects do not appear to play an important role.

**Synthesis of Catalysts 8d, 8f, and 8g and Determination of Their Experimental Selectivities for KR of Alcohol 9 with Isobutyric Anhydride.** Synthesis of these new analogues followed a synthetic route adapted from that used to make the parent catalyst **8a** starting from commercially available 4-pyridone and 1-bromo-2-naphthol and proceeding via triflate **12** (Scheme 3, for details, see Supporting Information).<sup>9a</sup>

**Scheme 3. Synthesis of Catalysts 8d, 8f, and 8g**



The initially prepared racemates were separated into their atropisomeric enantiomers by semi-preparative chiral stationary phase HPLC (CSP-HPLC) and the (*S<sub>a</sub>*) enantiomers obtained in >99.9% ee in all cases (for details see Supporting Information). The absolute configuration of these atropisomers was assigned by correlation of the Cotton effects in their circular dichroism (CD) spectra to that of the parent catalyst **8a**.<sup>9b</sup> Using these catalysts, a series of KR experiments using 1-(1-naphthyl)ethanol (**9**) under conditions comparable to those shown in Scheme 1 but using 1 equiv of isobutyric anhydride were performed, and the levels of conversion and selectivity determined by analytical CSP-HPLC (see Supporting Information). The catalyst containing the 3,5-dimethyl substituted phenyl group, compound **8d**, displayed a significantly higher level of selectivity ( $s = 27$ ) than the parent phenyl-substituted catalyst **8a** ( $s = 16$ ), whereas both the 4-methoxy- and 4-trifluoromethyl substituted catalysts **8f** and **8g** displayed lower levels of selectivity ( $s = 11$  and  $9$ , respectively, Table 3).

**Comparison between Experimental Selectivities and Theoretical Predictions.** With the experimentally measured selectivities  $s$  for the new catalysts **8d**, **8f**, and **8g** in hand, it is possible to quantify the predictive value of the theoretically calculated enthalpy differences  $\Delta H_{298}(S - R)$  (Table 3). The



enthalpy differences  $\Delta H_{298}(S - R)$  calculated at the B3LYP/6-31G(d) level can be correlated with experimental enantioselectivities (Figure 5, red line, correlation coefficient  $R^2 = 0.8792$  for catalysts **8a**, **8d**, **8f**, and **8g**). Figure 5 shows that the derivatives of catalyst **8a**, substituted in the phenyl ring, have a larger slope of the correlation line as compared to the catalysts **8a–c** and **8e**, which have different 4-dialkylamino substituents indicating that the 'blocking group' has a more decisive role in determining the selectivity of a catalyst than the 4-dialkylamino substituents. The thermal corrections recalculated at 195 K do not improve the correlation between experimental results and calculated enthalpies or free energies. Inclusion of dispersion corrections (at the B3LYP-D/6-311+G(d,p) level) slightly improves the overall correlation of experimental selectivities with calculated enthalpy differences for all studied catalysts **8a–g** (Table 3).

The experimental results are therefore consistent with the expectation from theory that 3,5-disubstitution enhances the enantioselectivity induced by the phenyl 'blocking group' in this class of catalyst, whereas 4-substitution does not.

**Experimental Deuterium Isotope Effects.** Mechanistic insight can often be provided by the study of deuterium isotope effects both by experiment and computation.<sup>24</sup> To this end, we have performed a series of experiments using the achiral PPY catalyst **11** and the enantiomerically pure catalysts **8a** and **8d** to compare the isobutyrylation of alcohols **9** and **d<sub>1</sub>-9** under otherwise identical conditions. Since all the key TSs [i.e., TS1-9, TS2, TS3, and TS4 for isobutyrylation using PPY (**11**, Figure 2) and (R)/(S)-TS1-9, (R)/(S)-TS2, (R)/(S)-TS3 for isobutyrylation using **8a** (Figure 3)] involve transfer of the hydrogen atom which is initially part of the alcohol hydroxyl group to the isobutyryl carboxylate, the introduction of a deuterium atom as in d<sub>1</sub>-1-(1-naphthyl)ethanol (**d<sub>1</sub>-9**) would be expected to significantly influence these reactions. The kinetic isotope effect (KIE) for isobutyrylation of alcohols **9** and **d<sub>1</sub>-9** catalyzed by PPY (**11**) was experimentally measured at  $-78^\circ\text{C}$  (see Supporting Information), and  $k_{\text{H}}/k_{\text{D}}$  found to be 2.64, which corresponds to a free energy difference of 1.58 kJ mol<sup>-1</sup>. Similarly, the KIEs for isobutyrylation of alcohols **9** and **d<sub>1</sub>-9** catalyzed by catalysts **8a** and **8d** were measured (Table 4).

The data reveal that changing from alcohol **9** to deuterated alcohol **d<sub>1</sub>-9** affects both the level of conversion and the level of enantioselectivity achieved in these catalyzed KR processes. The effect on enantioselectivity is most pronounced on the

parent catalyst **8a** ( $s_{\text{H}}/s_{\text{D}} = 1.92$ ,  $\Delta G_{\text{D-H}}(S - R) = 1.05$  kJ mol<sup>-1</sup>). On changing the phenyl substituent to the 3,5-(CH<sub>3</sub>)<sub>2</sub>C<sub>6</sub>H<sub>3</sub> substituent in the catalyst **8d** the drop in selectivity becomes smaller ( $s_{\text{H}}/s_{\text{D}} = 1.57$ ,  $\Delta G_{\text{D-H}}(S - R) = 0.74$  kJ mol<sup>-1</sup>). The effect on the level of conversion (i.e., rate of reaction) is marginal for both catalysts **8a** and **8d** ( $\Delta C_{(\text{H-D})} < 3\%$ ).

These experimental data imply that in all cases the rate-limiting TSs become slightly less stabilized (i.e., higher in energy and the overall rate is reduced) with deuterium replacing hydrogen but that the effect is more pronounced for the favored (R)-TS relative to the disfavored (S)-TS. Moreover, the differential effect of this on the two competing TSs is greatest for the parent catalyst **8a**.

Reliable computational modeling of these intriguing KIEs awaits experimental determination of detailed rate laws for the individual proton transfer events so as to allow appropriate combination of calculated KIEs for the corresponding TSs depicted in Figures 2 and 3.

## CONCLUSIONS

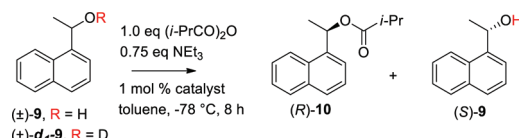
The rate accelerations provided by 4-DMAP-type catalysts in the acylation of alcohols by anhydrides are generally believed to be the result of a nucleophilic catalysis mechanistic reaction manifold. In this work, we have confirmed that the nucleophilic mechanism is more favorable than the general base mechanism for the reaction of 1-(1-naphthyl)ethanol (**9**) with isobutyric anhydride catalyzed by the achiral PPY catalyst **11** using computational methods (DFT at B3LYP/6-311+G(d,p)//B3LYP/6-31G(d) level). We have also examined catalysis of the same reaction when performed as a KR using the chiral 4-DMAP catalyst (–)-(S<sub>a</sub>)-**8a**. The TSs of the enantioselectivity-determining step have been identified for each enantiomer of the alcohol **9** and have been found to constitute four types in which the two alcohol enantiomers prefer different directions of approach to the key chiral acylpyridinium intermediate. The key TS models have also been used to predict the levels of enantioselectivity for two series of related catalysts differing in the dialkylamino substituent (catalysts **8a–c** and **8e**) and the aryl substitution pattern (catalysts **8a**, **8d**, **8f**, and **8g**), respectively. The successful validation of the predictions for highly selective catalyst **8d** further supports the mechanistic model chosen here; this and the trends with respect to the influence of the dialkyl amino and aryl 'blocking substituents' on enantioselectivity are anticipated to provide a platform for the future development of even more selective catalysts.<sup>23</sup>

The experimentally determined KIEs obtained in this work demonstrate for the first time that alcohol deuteration has a significant effect on the selectivity of these catalyzed alcohol KR reactions, and understanding these effects computationally is likely to provide additional important insight into the detailed energetics of proton transfer in the rate/selectivity-determining TSs of these processes. The current computational model cannot explain these results for this complex multi-TS system,<sup>24</sup> possibly due to inaccuracies in accounting for entropy<sup>25</sup> and/or handling tunneling effects<sup>26</sup> and asymmetry in proton-transfer<sup>27</sup> events. Work to overcome these limitations is planned and will be reported in due course.

## EXPERIMENTAL DETAILS

**General Procedure for the Isobutyrylation of 1-(1-naphthyl)ethanol (**9**) Catalyzed by PPY (**11**) (Scheme 2, Figure 1).** A solution of (±)-1-(1-naphthyl)ethanol **9** (2 mmol), NEt<sub>3</sub> (6

**Table 4. Influence of H-Bonding on KR of Alcohol **9** by Isobutyrylation Using Catalysts **8a** and **8d****



entry	catalyst	alcohol	C, % <sup>a</sup>	<i>s</i> <sup>b</sup>	$\Delta G(S - R)^c$	$\Delta G_{\text{D-H}}(S - R)^d$
1	(–)- <b>8a</b>	<b>9</b>	27	16	4.48	1.05
2	(–)- <b>8a</b>	<b>d<sub>1</sub>-9</b>	24	8.3	3.43	
3	(–)- <b>8d</b>	<b>9</b>	39	27	5.32	0.74
4	(+)- <b>8d</b>	<b>d<sub>1</sub>-9</b>	36	17	4.59 <sup>e</sup>	

<sup>a</sup>Conversion C was calculated from HPLC. <sup>b</sup>Selectivity factor *s* was determined using Kagan's equation.<sup>22</sup> <sup>c</sup> $\Delta G(S - R)$  (kJ mol<sup>-1</sup>) was calculated using eq 1 at  $T = 195.15$  K. <sup>d</sup> $\Delta G_{\text{D-H}}(S - R) = \Delta G_{\text{D}}(S - R) - \Delta G_{\text{H}}(S - R)$  (kJ mol<sup>-1</sup>). <sup>e</sup>As the antipodal catalyst was used in this experiment, the values are for  $\Delta G(R - S)$  rather than  $\Delta G(S - R)$ .



mmol), 1,3,5-trimethoxybenzene (0.33 mmol), and PPY (**11**, 0.5 mol %) in toluene (8 mL) was cooled to  $-78^{\circ}\text{C}$ . (*i*-PrCO)<sub>2</sub>O (4 mmol) was added dropwise with vigorous stirring. Every 10–30 min, an aliquot of the reaction mixture (50  $\mu\text{L}$ ) was carefully removed and quenched with MeOH (1 mL). The solvents were distilled off under reduced pressure, and  $^1\text{H}$  NMR spectra were measured. The signals of the ester **10** at  $\delta$  6.64 ppm and the alcohol **9** at  $\delta$  5.70 ppm were integrated, and the conversion  $y$  is given by eq 2:

$$y = \frac{I_{\text{ester}}}{I_{\text{ester}} + I_{\text{ROH}}} \cdot 100\% \quad (2)$$

Dependence of the conversion  $y$  vs time  $t$  was fitted by eq 3 for second-order reaction kinetics:

$$y = y_0 \left( 1 - \frac{1}{2e^{k(t-t_0)} - 1} \right) \quad (3)$$

$$k = k_2[\text{ROH}]_0 \quad (4)$$

where  $k_2$  is a rate-constant of the second-order reaction and  $t_0$  has a meaning of time axis offset. With this parameter in the fitting process, it is not necessary to measure the starting point of the reaction exactly. The variable  $y_0$  allows for rescaling of the conversion axis. The rate constants were measured two times and then averaged (see Supporting Information for full information).

**General Procedure for the KR of 1-(1-naphthyl)ethanol (**9**) Using Isobutyric Anhydride Catalyzed by Chiral-DMAP Catalysts **8a**, **8d**, **8f**, and **8g** (Table 3).** All KR experiments were run in duplicate. An oven-dried microwave glass vial (0.5–2.0 mL capacity, 1.25 cm I.D.  $\times$  8.0 cm L, Biotage Ltd.) equipped with a Teflon magnetic stirring bar (Biotage Ltd.) was charged with (–)-{3-[2-(3,5-dimethylphenyl)naphthalen-1-yl]pyridin-4-yl}diethylamine **8d** (0.0038 g, 0.01 mmol, 0.01 equiv) and 1-(1-naphthyl)ethanol **9** (0.1722 g, 1.0 mmol, 1.0 equiv). The vial was sealed with an airtight aluminum/rubber septum (Reseal design, Biotage Ltd.) using a crimper. The contents in the vial were dried in vacuo and purged with argon gas ( $\times 3$ ). Dry toluene (2 mL) and dry  $\text{NEt}_3$  (0.105 mL, 0.75 mmol, 0.75 equiv) were added to the vial under an argon atmosphere, and the mixture was stirred on an isopropanol bath which was maintained at a constant  $-78^{\circ}\text{C}$  using a cryostat. After 30 min, isobutyric anhydride (0.166 mL, 1.0 mmol, 1.0 equiv) was added to the reaction mixture under an argon atmosphere, and the mixture was stirred ( $\sim 1000$  rpm) at  $-78^{\circ}\text{C}$ . After 2 h, 1 mL of the reaction mixture was drawn out using a syringe and rapidly transferred into a sealed vial (Biotage as described above) containing a magnetic stirring bar and methanol (2 mL/0.5 mmol of substrate) that has been precooled to  $-78^{\circ}\text{C}$  for at least 1 h under an argon atmosphere. The remainder of the reaction mixture was continued to be stirred at  $-78^{\circ}\text{C}$  for an additional 6 h (total time = 8 h), after which it was quenched with cold methanol (2 mL) that was precooled at  $-78^{\circ}\text{C}$  as described above. Each of the reaction mixtures were then stirred and allowed to warm to r.t. overnight [Note: Abrupt warming of the reaction mixture during the quenching process must be avoided]. After the quenching process was complete, each of these reaction mixtures was quickly evaporated to dryness under reduced pressure, and the crude material was subjected to flash chromatography on  $\text{SiO}_2$  [eluent:  $\text{CH}_2\text{Cl}_2$ /*n*-hexane (1:1) then  $\text{CH}_2\text{Cl}_2$ ] to give ester **10** (0.018 g, 15% for 2 h reaction; 0.046 g, 38% for 8 h reaction) as a colorless oil and unreacted alcohol **9** [0.072 g, 84% (recovered isolated yield) for the 2 h reaction; 0.052 g, 60% (recovered isolated yield) for the 8 h reaction] as a white solid. The spectroscopic and analytical data of the unreacted alcohol **9** and ester **10** were consistent with those reported in the literature.<sup>9a</sup> Analysis of the enantiomeric purity of the alcohol **9** was performed directly, whereas that of the ester **10** was performed after hydrolysis to the alcohol **9**, as described below.

**Saponification of Ester **10**.** The ester **10** obtained from each KR experiment was hydrolyzed by heating to reflux in 5% NaOH/MeOH (2 mL for 0.5 mmol substrate) for 5 min. After evaporation of the solvent, the residue was subject to rapid flash chromatography ( $\text{SiO}_2$ ) eluting with  $\text{CH}_2\text{Cl}_2$  to give the hydrolyzed alcohol **9** as a white solid

(quantitative yield). The enantiomeric excess for the unreacted alcohol **9** and the alcohol obtained by the ester saponification (**10**  $\rightarrow$  **9**) was established by analytical CSP HPLC using Chiralcel OD-H (0.46 cm I.D.  $\times$  25 cm L; 5  $\mu\text{m}$  silica). Mobile phase: *n*-hexane/2-propanol, 90/10; flow rate: 1 mL  $\text{min}^{-1}$ ; temperature:  $35^{\circ}\text{C}$ ; sample conc. = 2 mg/mL in 2-propanol; and injection: 1 or 2  $\mu\text{L}$ . Each sample was analyzed at least twice to obtain concordant ee values (see Supporting Information).

## ■ ASSOCIATED CONTENT

### Supporting Information

Synthetic procedures, characterization data of new compounds, procedures of the KR, computational data, and complete ref 15. This material is available free of charge via the Internet at <http://pubs.acs.org>.

## ■ AUTHOR INFORMATION

### Corresponding Author

[zipse@cup.uni-muenchen.de](mailto:zipse@cup.uni-muenchen.de); [a.c.spivey@imperial.ac.uk](mailto:a.c.spivey@imperial.ac.uk)

### Present Addresses

<sup>§</sup>MRC Laboratory of Molecular Biology, Hills Road, Cambridge, CB2 0QH, United Kingdom.

<sup>||</sup>Department of Organic Chemistry, University of Geneva, Quai Ernest Ansermet 30, Geneva, Switzerland.

<sup>†</sup>State Key Laboratory of Organometallic Chemistry, Shanghai Institute of Organic Chemistry, Chinese Academy of Sciences, 345 Lingling Road, Shanghai 200032 China.

### Notes

The authors declare no competing financial interest.

## ■ ACKNOWLEDGMENTS

Synthetic aspects of the work described in this manuscript were supported by a grant from the EPSRC (GR/S04284/01). Theoretical and mechanistic aspects have been supported by a grant of the Deutsche Forschungsgemeinschaft (DFG) in the focus program SPP 1179 “Organocatalysis” (ZI 439/10).

## ■ REFERENCES

- (1) (a) Höfle, G.; Steglich, W.; Vorbrüggen, H. *Angew. Chem.* **1978**, 90, 602; *Angew. Chem., Int. Ed. Engl.* **1978**, 17, 569. (b) Spivey, A. C.; Arseniyadis, S. *Angew. Chem.* **2004**, 116, 5552; *Angew. Chem., Int. Ed. Engl.* **2004**, 43, 5436.
- (2) (a) Vedejs, E.; Jure, M. *Angew. Chem., Int. Ed.* **2005**, 44, 3974. (b) Wurz, R. *Chem. Rev.* **2007**, 107, 5570. (c) Spivey, A. C.; McDaid, P. *Asymmetric Acyl Transfer Reactions. In Handbook of Asymmetric Organocatalysis*; Dalko, P., Ed.; Wiley-VCH, Weinheim, Germany, 2007, pp 287–329. (d) Spivey, A. C.; Arseniyadis, S. *Top. Curr. Chem.* **2010**, 291, 233. (e) Müller, C. E.; Schreiner, P. R. *Angew. Chem., Int. Ed.* **2011**, 50, 6012.
- (3) (a) Vedejs, E.; Chen, X. *J. Am. Chem. Soc.* **1996**, 118, 1809. (b) Vedejs, E.; Chen, X. *J. Am. Chem. Soc.* **1997**, 119, 2584. (c) Duffey, T. A.; MacKay, J. A.; Vedejs, E. *J. Org. Chem.* **2010**, 75, 4674.
- (4) (a) Kawabata, T.; Nagato, M.; Takasu, K.; Fuji, K. *J. Am. Chem. Soc.* **1997**, 119, 3169. (b) Kawabata, T.; Yamamoto, K.; Momose, Y.; Yoshida, H.; Nagaoka, Y.; Fuji, K. *Chem. Commun.* **2001**, 2700. (c) Kawabata, T.; Stragies, R.; Fukaya, T.; Nagaoka, Y.; Schedel, H.; Fuji, K. *Tetrahedron Lett.* **2003**, 44, 1545. (d) Kawabata, T.; Stragies, R.; Fukaya, T.; Fuji, K. *Chirality* **2003**, 15, 71–76. (e) Muramatsu, W.; Kawabata, T. *Tetrahedron Lett.* **2007**, 48, 5031. (f) Kawabata, T.; Muramatsu, W.; Nishio, T.; Shibata, T.; Uruno, Y.; Stragies, R. *Synthesis* **2008**, 747.
- (5) (a) Ruble, J. C.; Fu, G. C. *J. Am. Chem. Soc.* **1998**, 120, 11532. (b) Tao, B.; Ruble, J. C.; Hoic, D. A.; Fu, G. C. *J. Am. Chem. Soc.* **1999**, 121, 5091. (c) Fu, G. C. *Acc. Chem. Res.* **2000**, 33, 412. (d) Fu, G. C.; Ie, Y. *Chem. Commun.* **2000**, 119. (e) Arai, S.; Bellemine-Lapponnaz, S.;

Fu, G. C. *Angew. Chem., Int. Ed.* **2001**, *40*, 234. (f) Fu, G. C. *Acc. Chem. Res.* **2004**, *37*, 542. (g) Arp, F. O.; Fu, G. C. *J. Am. Chem. Soc.* **2006**, *128*, 14264. (h) Wurz, R. P.; Lee, E. C.; Ruble, J. C.; Fu, G. C. *Adv. Synth. Cat.* **2007**, *349*, 2345.

(6) (a) Naraku, G.; Shimomoto, N.; Hanamoto, T.; Inanaga, J. *Enantiomer* **2000**, *5*, 135. (b) Kotsuki, H.; Sakai, H.; Shinohara, T. *Synlett* **2000**, 116. (c) Priem, G.; Anson, M. S.; Macdonald, S. J. F.; Pelotier, B.; Campbell, I. B. *Tetrahedron Lett.* **2002**, *43*, 6001. (d) Jeong, K.-S.; Kim, S.-H.; Park, H.-J.; Chang, K.-J.; Kim, K. S. *Chem. Lett.* **2002**, *31*, 1114. (e) Priem, G.; Pelotier, B.; Macdonald, S. J. F.; Anson, M. S.; Campbell, I. B. *J. Org. Chem.* **2003**, *68*, 3844. (f) Pelotier, B.; Priem, G.; Campbell, I. B.; Macdonald, S. J. F.; Anson, M. S. *Synlett* **2003**, 679. (g) Pelotier, B.; Priem, G.; Macdonald, S. J. F.; Anson, M. S.; Upton, R. J.; Campbell, I. B. *Tetrahedron Lett.* **2005**, *46*, 9005. (h) Yamada, S.; Misono, T.; Iwai, Y. *Tetrahedron Lett.* **2005**, *46*, 2239. (i) Dalaigh, C. O.; Hynes, S. J.; Maher, D. J.; Connon, S. J. *Org. Biomol. Chem.* **2005**, *3*, 981. (j) Diez, D.; Gil, M. J.; Moro, R. F.; Garrido, N. M.; Marcos, I. S.; Basabe, P.; Sanz, F.; Broughton, H. B.; Urones, J. G. *Tetrahedron: Asymm.* **2005**, *16*, 2980. (k) Poisson, T.; Penhoat, M.; Papamicaël, C.; Dupas, G.; Dalla, V.; Marsais, F.; Levacher, V. *Synlett* **2005**, 2285. (l) Yamada, S.; Misono, T.; Iwai, Y.; Masumizu, A.; Akiyama, Y. *J. Org. Chem.* **2006**, *71*, 6872. (m) Dalaigh, C. O.; Hynes, S. J.; O'Brien, J. E.; McCabe, T.; Maher, D. J.; Watson, G. W.; Connon, S. J. *Org. Biomol. Chem.* **2006**, *4*, 2785. (n) Yamada, S.; Yamashita, K. *Tetrahedron Lett.* **2008**, *49*, 32. (o) Šámal, M.; Mišek, J.; Stará, I. G.; Starý, I. *Collect. Czech. Chem. Commun.* **2009**, *74*, 1151. (p) Crittall, M. R.; Rzepa, H. S.; Carbery, D. R. *Org. Lett.* **2011**, *13*, 1250.

(7) (a) Birman, V. B.; Uffman, E. W.; Jiang, H.; Li, X.; Kilbane, C. J. *J. Am. Chem. Soc.* **2004**, *126*, 12226. (b) Birman, V. B.; Jiang, H. *Org. Lett.* **2005**, *7*, 3445. (c) Birman, V. B.; Li, X.; Jiang, H.; Uffman, E. W. *Tetrahedron* **2006**, *62*, 285. (d) Birman, V. B.; Li, X. *Org. Lett.* **2006**, *8*, 1351. (e) Birman, V. B.; Guo, L. *Org. Lett.* **2006**, *8*, 4859. (f) Iwai, Y.; Jiang, H.; Li, X. *Org. Lett.* **2007**, *9*, 3237. (g) Birman, V. B.; Li, X. *Org. Lett.* **2008**, *10*, 1115. (h) Li, X.; Liu, P.; Houk, K. N.; Birman, V. B. *J. Am. Chem. Soc.* **2008**, *130*, 13836. (i) Li, X.; Jiang, H.; Uffman, E. W.; Guo, L.; Zhang, Y.; Yang, X.; Birman, V. B. *J. Org. Chem.* **2012**, *77*, 1722.

(8) (a) Shiina, I.; Nakata, K. *Tetrahedron Lett.* **2007**, *48*, 8314. (b) Shiina, I.; Nakata, K.; Onda, Y.-s. *Eur. J. Org. Chem.* **2008**, 5887. (c) Xu, Q.; Zhou, H.; Geng, X.; Chen, P. *Tetrahedron* **2009**, *65*, 2232. (d) Shiina, I.; Nakata, K.; Sugimoto, M.; Onda, Y.-s.; Iizumi, T.; Ono, K. *Heterocycles* **2009**, *77*, 801. (e) Shiina, I.; Nakata, K.; Ono, K.; Sugimoto, M.; Sekiguchi, A. *Chem.—Eur. J.* **2010**, *16*, 167. (f) Shiina, I.; Nakata, K.; Ono, K.; Onda, Y.-s.; Itagaki, M. *J. Am. Chem. Soc.* **2010**, *132*, 11629. (g) Hu, B.; Meng, M.; Wang, Z.; Du, W.; Fossey, J. S.; Hu, X.; Deng, W.-P. *J. Am. Chem. Soc.* **2010**, *132*, 17041. (h) Wagner, A. J.; David, J. G.; Rychnovsky, S. D. *Org. Lett.* **2011**, *13*, 4470. (i) Belmessieri, D.; Joannes, C.; Woods, P. A.; MacGregor, C.; Jones, C.; Campbell, C. D.; Johnston, C. P.; Duguet, N.; Concellon, C.; Bragg, R. A.; Smith, A. D. *Org. Biomol. Chem.* **2011**, *9*, 559. (j) Viswambharan, B.; Okimura, T.; Suzuki, S.; Okamoto, S. *J. Org. Chem.* **2011**, *76*, 6678.

(9) (a) Spivey, A.; Fekner, T.; Spey, S. E. *J. Org. Chem.* **2000**, *65*, 3154. (b) Spivey, A. C.; Zhu, F.; Mitchell, M. B.; Davey, S. G.; Jarvest, R. L. *J. Org. Chem.* **2003**, *68*, 7379. (c) Spivey, A. C.; Leese, D. P.; Zhu, F.; Davey, S. G.; Jarvest, R. L. *Tetrahedron* **2004**, *60*, 4513. (d) Spivey, A. C.; Arseniyadis, S.; Fekner, T.; Maddaford, A.; Leese, D. P. *Tetrahedron* **2006**, *62*, 295.

(10) Upon reinvestigation in this work, the selectivity factor  $s = 24$  reported in refs 9a and 9c for catalyst (–)-(S<sub>d</sub>)-**8a** in the KR corresponding to Scheme 1 (and the value  $s = 29$  for the analogous reaction using just 1 equiv of anhydride, see ref 9a) was found to be incorrect as the result of HPLC integration errors arising from an impurity co-running with one enantiomer of the alcohol **9**. The correct values should be  $s = 16$  for both cases. Additionally, the selectivity factor  $s = 9$  reported in ref 9c for catalyst (–)-(S<sub>d</sub>)-**8i** was a typo and should have read  $s = 39$ ; this value was however obtained in a KR experiment run at –93 °C over 14.3 h (cf. –78 °C and 9 h for all other

entries in Scheme 1) and so is not directly comparable to the others listed.

(11) Wei, Y.; Held, I.; Zipse, H. *Org. Biomol. Chem.* **2006**, *4*, 4223.

(12) (a) Shinisha, C. B.; Sunoj, R. B. *Org. Lett.* **2009**, *11*, 3242. (b) Müller, C. E.; Wanka, L.; Jewell, K.; Schreiner, P. R. *Angew. Chem., Int. Ed.* **2008**, *47*, 6180.

(13) (a) Jorgensen, W. L.; Tirado-Rives, J. *J. Comput. Chem.* **2005**, *26*, 1689. (b) Jorgensen, W. L.; Maxwell, D. A.; Tirado-Rives, J. *J. Am. Chem. Soc.* **1996**, *118*, 11225.

(14) Xu, S.; Held, I.; Kempf, B.; Mayr, H.; Steglich, W.; Zipse, H. *Chem.—Eur. J.* **2005**, *11*, 4751.

(15) Frisch, M. J., et al. *Gaussian 03*, revision D.01; Gaussian, Inc.: Pittsburgh, PA, 2004.

(16) (a) Grimme, S. *J. Comput. Chem.* **2006**, *27*, 1787. (b) Grimme, S. *J. Comput. Chem.* **2004**, *25*, 1463–1473.

(17) Neese, F. *ORCA 2.6.4, an ab initio density functional and semiempirical program package*, 2007.

(18) (a) Satyanarayana, T.; Kagan, H. B. *Tetrahedron* **2007**, *63*, 6415. (b) Keith, J. M.; Larrow, J. F.; Jacobsen, E. N. *Adv. Synth. Catal.* **2001**, *343*, 5.

(19) Vedejs, E.; Daugulis, O.; Harper, L. A.; MacKay, J. A.; Powell, D. R. *J. Org. Chem.* **2003**, *68*, 5020.

(20) For discussion of activation parameters for nucleophilic catalysis in acyl-transfer reactions, see: (a) Oakenfull, D. G.; Riley, T.; Gold, V. *Chem. Commun.* **1966**, 385. (b) Miltien, J. B.; Fife, T. H. *J. Am. Chem. Soc.* **1968**, *90*, 2164. (c) Schowen, R. L.; Behn, C. G. *J. Am. Chem. Soc.* **1968**, *90*, 5839. (d) Butler, A. R.; Robertson, I. H. *J. Chem. Soc., Perkin Trans. 2* **1975**, 660.

(21) Bonduelle, C.; Martín-Vaca, B.; Cossío, F. P.; Bourissou, D. *Chem.—Eur. J.* **2008**, *14*, 5304.

(22) Kagan, H. B.; Fiaud, J. C. *Top. Stereochem.* **1988**, *18*, 249.

(23) From the trends established herein with respect to the influence of the 4-dialkylamino and aryl blocking groups on catalyst selectivity, it would be anticipated that the catalyst combining both 4-NBu<sub>2</sub> and 3,5-(CH<sub>3</sub>)<sub>2</sub>C<sub>6</sub>H<sub>3</sub> groups would exhibit high levels of selectivity. This is indeed the case. For the KR of alcohol **9** under conditions identical to those used in Table 3 for catalysts **8d**, **8f**, and **8g** [i.e., 8 h, –78 °C, toluene, 1 equiv (*i*-PrCO)<sub>2</sub>O, 0.75 equiv Et<sub>3</sub>N, 1 mol% cat], this catalyst displays a  $s$  value of 44 ( $C = 48.2\%$ ). The synthesis and scope of this catalyst for the KR of various alcohols will be the subject of a forthcoming communication.

(24) Giagou, T.; Meyer, M. P. *J. Org. Chem.* **2010**, *75*, 8088.

(25) O'Leary, D. J.; Hickstein, D. D.; Hansen, B. K. V.; Hansen, P. E. *J. Org. Chem.* **2010**, *75*, 1331.

(26) Nagel, Z. D.; Klinman, J. P. *Chem. Rev.* **2010**, *110*, P45.

(27) Stoyanov, E. S.; Stoyanova, I. V.; Reed, C. A. *J. Am. Chem. Soc.* **2010**, *132*, 1484.